Available online at www.sciencedirect.com
SCIENCE DIRECT®
Lithos 68 (2003) 121–130
LITHOS
www.elsevier.com/locate/lithos

Discussion

Reply to comments by Y. Zhu: K-feldspar in clinopyroxene from Grt-Cpx silicate rocks of the Kokchetav Massif☆

L.L. Perchuk[a,b,*], O.G. Safonov[a,b], V.O. Yapaskurt[a,b], J.M. Barton Jr.[c]

[a] Department of Petrology, Moscow State University, Moscow 119899, Russia
[b] Institute of Experimental Mineralogy of Russian Academy of Sciences, Chernogolovka, Moscow, District 142432, Russia
[c] Department of Geology, Rand Afrikaans University, P.O. Box 524, Auckland Park, Johannesburg 2006, South Africa

Received 25 July 2002; accepted 14 March 2003

1. Introduction

During the past decade, the origin of potassium feldspar (*Kfs*) in ultrahigh-pressure (UHP) rocks has drawn the attention of many workers because *Kfs* only occurs as blebs and microveins in clinopyroxene (*Cpx*) and never is associated with other minerals. The *Cpx*+*Kfs* paragenesis occurs in eclogitic nodules from kimberlitic pipes (cf. Reid et al., 1976) and in the UHP metamorphic rocks of the Kokchetav Massif, Siberia (e.g., Sobolev and Shatsky, 1990; Perchuk et al., 1995; Zhang et al., 1997). Superficially, the *Cpx*+*Kfs* paragenesis appears similar in rocks of different origins and compositions. However, detailed studies show that the composition of *Cpx*, the shape of the *Kfs* blebs and their distribution in the *Cpx* host are different in the rocks of different origin. We demonstrated wide variations of potassium content in *Cpx* from the specific Fe-rich, diamond-free, coarse-grained garnet (*Grt*)-*Cpx* rocks from the Kumdy-Kol Mine in the Kokchetav Complex (Perchuk et al., 1996; 2002; Bindi et al., 2003). The K_2O content in cores and centres of K-*Cpx* inclusions in garnet is nearly constant, but drops dramatically at their rims. We explained this sharp decrease by simultaneous crystallization of *Kfs* with new generation of the *Cpx* (*Cpx*2). The K_2O concentration in *Cpx*2 is similar to that of the low potassium *Cpx*1. Therefore, the *Cpx*2 should contain more *Kfs* blebs. *Kfs* blebs of different shapes, comprising 4–5 vol.%, are observed in the central portions of the *Cpx*2 grains, while *Kfs* blebs never occur in potassium-free, *Cpx* coronas (*Cpx*3).

The systematic zoning and sequence of crystallization of minerals in the rocks led us to conclude that they originally crystallized from a silicate melt at a depth of about 200 km. Subsequent evolution of these rocks resulted from ascent and cooling (Perchuk et al., 2002). However, in addition to K-*Cpx*, *Grt* also contains small, well-preserved carbonate inclusions; moreover, calcite likewise occurs in the matrix. Based on these observations, we suggested an initial coexistence of separate carbonate and silicate melts but did not comment on the primary nature of these melts (Perchuk et al., 2002).

The crystallization of potassium-bearing clinopyroxene (K-*Cpx*) at the liquidus in diverse silicate and carbonate–silicate systems is supported by the results

☆ doi of original article 10.1016/S0024-4937(03)00033-1.

* Corresponding author. Department of Petrology, Moscow State University, Moscow 119899, Russia. Tel.: +7-70959391305; fax: +7-70959328889.
E-mail addresses: llp@geol.msu.ru (L.L. Perchuk), oleg@iem.ac.ru (O.G. Safonov), jmb@na.rau.ac.za (J.M. Barton).

0024-4937/03/$ - see front matter
doi:10.1016/S0024-4937(03)00034-3

of UHP experiments (Edgar and Vukadinovic, 1993; Mitchell, 1995; Edgar and Mitchell, 1997), including those systems whose compositions are close to those of the Kokchetav rocks (Safonov et al., 2002). The origin of the *Kfs* blebs within *Cpx*2 suggests the reaction:

$$KAlSi_2O_6(\text{in } Cpx) + [SiO_2]_{melt} \Rightarrow KAlSi_3O_8 \quad (1)$$

or

$Ca(Fe,Mg)Si_2O_6 \cdot nKAlSi_2O_6$ (in *Cpx*)$+[SiO_2]_{melt} \Rightarrow nKAlSi_3O_8 + Ca(Fe,Mg)Si_2O_6$ because no eskolaite (*Esk*) component ($Ca_{0.5}\square_{0.5}AlSi_2O_6$) was observed in numerous *Cpx*2 analyses. It should be mentioned that we thoroughly tested the "*Esk* reaction" (Luth, 1997) in application to the formation of *Cpx*2 + *Kfs* assemblage and concluded that "... *KCpx* (*Cpx*1) from garnet-Cpx rocks of the Kokchetav Complex does not contain the *Esk* end-member" (Perchuk and Yapaskurt, 1998; Perchuk et al., 2002, p. 103). Therefore, the reaction:

$$3KAlSi_2O_6 + 2Ca_{0.5}\square_{0.5}AlSi_2O_6 = 3KAlSi_3O_8 + CaAl_2SiO_6 \quad (2)$$

or K-*Jadeite* in *Cpx* (K-*Jad*) + Ca-*Eskola end member* (*Esk*) = K-*feldspar* (*Kfs*) + Ca-*Tschermakite* (*Tsch*) is not valid for the diamond-free, coarse-grained rocks occurring in the Kumdy-Kol Mine.

Presumably, Zhu (2003) did not read our paper (Perchuk et al., 2002) carefully and therefore incorrectly understood our conclusion about the origin of *Kfs* blebs in the *Cpx*2. This appears to be the only

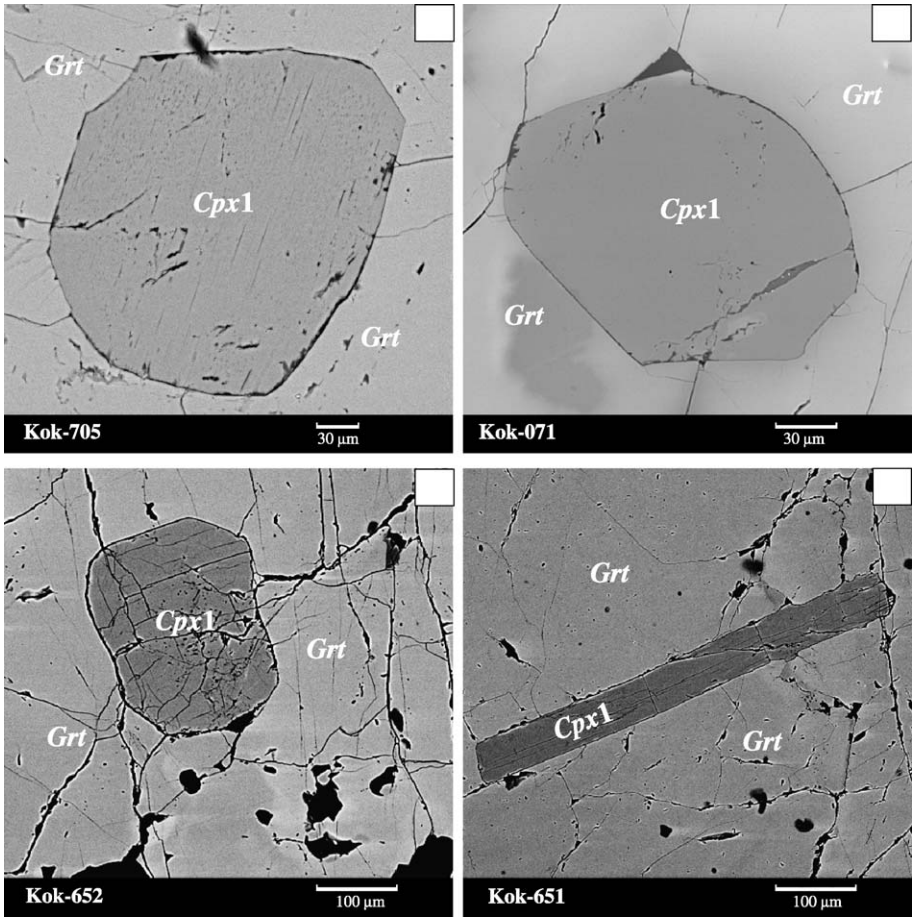

Fig. 1. Backscattered images of potassium-bearing *Cpx* included into garnet of the Fe-rich, diamond-free, coarse-grained *Grt-Cpx* rock from the Kumdy-Kol Mine, the Kokchetav Complex. No *Kfs* blebs are present.

reason for their criticism of our idea concerning the role of reaction (1) in the formation of *Kfs* blebs. On the other hand, the comments of Zhu allow us to expand our discussion of this very interesting problem.

2. The rock types discussed

In our papers we outlined the above rock type in which the K-rich *Cpx*1 at liquidus is changed by the crystallization of the *Cpx*2 with the *Kfs* blebs (Perchuk et al., 1996; 2002). These rocks occur as large boudins and lenses in *Grt-Bio* diamondiferous gneisses. Major rock-forming minerals in these boudins and lenses are Fe–Ca garnet ($X^{Grt}_{Mg}=0.05–0.15$; $X^{Grt}_{Ca}=0.75–0.80$) and *Cpx* ($X^{Cpx}_{Mg}=0.4–0.6$). Primary garnet contains inclusions of the euhedral K-*Cpx* (Fig. 1). This K-*Cpx* shows systematic chemical zoning (Perchuk et al., 2002). Primary K-*Cpx* never coexists with *Kfs*. *Cpx*2 forms large, up to centimeter in size, porphyroblasts (or porphyroclasts?) and rare euhedral fine grains included in *Grt* containing *Kfs* blebs (Fig. 2a and b). On one hand, the *Kfs* inclusions in garnet (Fig. 2a) suggest that the crystallization of garnet continues after the formation of *Cpx*2, and on the other, *Kfs* blebs are not the products of the *Cpx*1 exsolution. The *Cpx*3 which does not contain *Kfs* blebs surrounds *Cpx*2 (Fig. 2b). In some samples, *Cpx*2 porphyroblasts contain rare quartz inclusions of 5–10 μm in size, amounting to less than 1 vol.%. Besides the blebs and intergrowths, *Kfs* occurs as late (*Kfs*2) microveins crosscutting all generations of *Cpx* (Perchuk et al., 2002). The *Kfs* of all generations is pure orthoclase. Outside of the porphyroblasts, *Cpx*3 forms intergrowths with *Kfs* (Fig. 2b), resembling eutectic relationships. Titanite and rutile are common primary accessories in the rocks. No epidote, chlorite nor albite occur either in blebs within *Cpx*2, or in any other primary form.

Thus, the mineral and bulk compositions of the Fe-rich *Cpx-Grt* silicate rocks discussed in our papers (Perchuk et al., 1996; 2002) strongly differ from those in the Mg-rich *marble* described in Zhu's paper. Although we never mentioned a protholith of the rock, Zhu attributes to us the idea that the formation of the *Cpx-Grt* bearing silicate rock resulted from "melting of a metamorphic rock." We have to reiterate that the Kumdy-Kol Mine portion of the Kokchetav massif is characterized by different types of magmatic and metamorphic UHP rocks. Therefore, in order to make a decision on the origin of *Kfs* blebs in silicate rocks, we cannot use compositional and textural characteristics of metamorphic rocks. The comparison of chemistry of *Cpx* occurring in silicate rocks (our case) and those occurring in carbonate rocks (Zhu's case) has no significance.

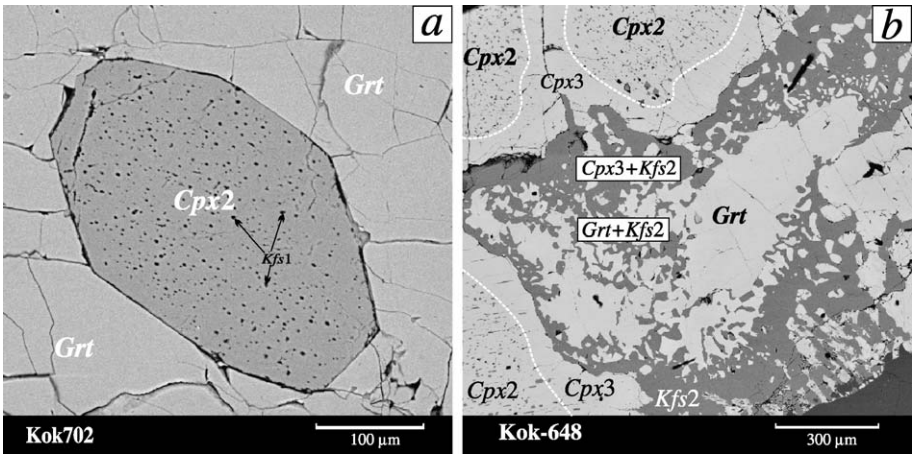

Fig. 2. Backscattered images of *Cpx*2 and *Cpx3* in the Fe-rich, diamond-free, coarse-grained *Grt-Cpx* rock from the Kumdy-Kol Mine, the Kokchetav Complex. (a) Very fine inclusions of *Kfs* in *Cpx*2 included in garnet. (b) Mineral zoning around garnet: (1) symplectites of *Grt* with *Kfs*2, (2) symplectites of *Cpx*2 with *Kfs*2, and (3) the *Kfs* blebs-free *Cpx*3 coronas.

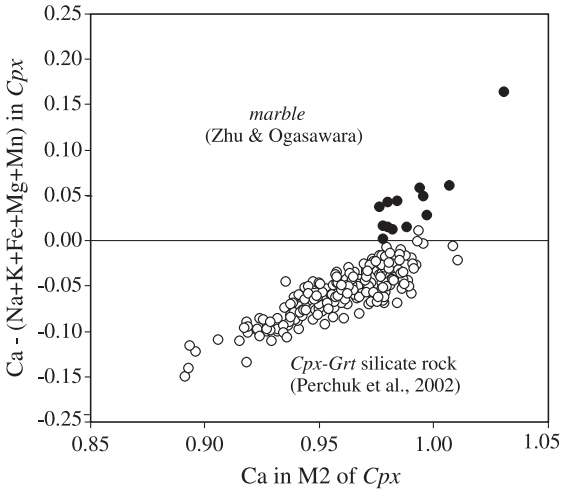

Fig. 3. The diagram demonstrating principal difference between compositions of *Cpx* from silicate rock (Perchuk et al., 1996; 2002) and marble (Zhu, 2003) in terms of Ca content in the M2 site. Open circles represent data points of *Cpx* from silicate rock (Perchuk et al., 1996, 2002); closed circles represent data points of *Cpx* from marble (Zhu, 2003).

In order to test the models in terms of reaction (2), we must compare the predominant substitution mechanisms in K-*Cpx* (*Cpx*1) and *Cpx*2. *Cpx*1 and the *Cpx*2 from marbles "…are characterized by higher content of Ca" (Dobretsov et al., 1971, p. 176) that completely occupies the M2 site. Fig. 3 illustrates this pattern, while the *Cpx* from *Grt-Cpx* bearing silicate rock show a lack of Ca with respect to K, Na, Fe and Mg, suggesting saturation of the M2 site by K and Na instead of Ca with the charge compensation by Al and Fe^{3+} in the M1 site. The excess Ca in the M2 site of *Cpx*1 from marble (Fig. 3) suggests that the *Esk* component is not characteristic of the primary *Cpx* in the rock.

Any model addressing the formation of K-*Cpx* must demonstrate clear evidence for (Fe, Mg)Si_2O_6–$KAlSi_2O_6$ solid solution in *Cpx*1. Furthermore, in order to use reaction (2), the $Ca_{0.5}\square_{0.5}AlSi_2O_6$ component in the primary *Cpx*1 must occur, while *Cpx*2, the product of reaction (2), (i) must be *Tsch*-rich and (ii) must contain *Kfs* blebs.

3. Cpx from the silicate rock

From our observations, *Cpx* crystallized in three generations. The first one, K-*Cpx* (Perchuk et al., 1995; 1996), occurs as inclusions in garnet, and never contains *Kfs* blebs. *Cpx*2 contains little or no potassium (Perchuk et al., 2002) but contains up to 4–5 vol.% *Kfs* blebs. *Cpx*3 surrounds *Cpx*2, and contains neither K_2O nor *Kfs* blebs. However, it forms symplectites with orthoclase (Fig. 2). Thus, all three generations of *Cpx* differ in morphology, and presumably, in chemical composition. Apart from a brief discussion by Perchuk et al. (1995), a significant number of chemical analyses of all three generations of *Cpx* have not been published. We take this opportunity to do so.

Most of the *Cpx* compositions were determined using a CamScan electron microscope fitted with a well-standardized EDS Link AN10/85S (Department of Petrology, Moscow State University). Additional analyses were made using a wave-length Camebax SX50 instrument at the Institute of Experimental Mineralogy and a JEOL JXA 8600 instrument at the Dipartimento di Scienze della Terra, Università di Firenze. More than 130 and 110 probe analyses were produced for *Cpx*1 and *Cpx*2, respectively, as well as a few dozen analyses of *Cpx*3. Representative analyses of all three generations of *Cpx* from coarse grained *Grt-Cpx* silicate rocks from the Kumby-Kol Mine are shown in the Table 1.

The following scheme was applied to recalculate the *Cpx* formula (per 6 oxygen atoms) for site occupancy: Al^T=2-Si, Al^{M1}=Al–Al^T, Fe^{3+}=Na-(Al-2·

$Al^{T}-K)-2\cdot Ti$, $(Mg+Fe)^{M1}=1-(Al^{M1}+Cr+Ti+Fe^{3+})$, $Mg^{M1}=X_{Mg}^{Cpx}\cdot(Mg+Fe)^{M1}$, $Fe^{M1}=(1-X_{Mg}^{Cpx})\cdot(Mg+Fe)^{M1}$ (tentatively assuming uniform distribution of Mg and Fe between M1 and M2), $Mg^{M2}=Mg-Mg^{M1}$, $Fe^{M2}=Fe-Fe^{M1}$, $\square^{M2}=1-(Ca+Na+K+Mn+Mg^{M2}+Fe^{M2})$. Admitting that $\square^{M2}$ can be compensated via the introduction of other cations in M1 (i.e., Cr, Fe^{3+}) in addition to Al^{M1} to form *Esk*-like components ($Ca_{0.5}\square_{0.5}AlSi_2O_6$, $Ca_{0.5}\square_{0.5}FeSi_2O_6$, $Ca_{0.5}\square_{0.5}CrSi_2O_6$), we have calculated an excess cations in M1 over $KAlSi_2O_6$, $NaAlSi_2O_6$, $CaAl_2SiO_6$, $NaFeSi_2O_6$, etc.: $(Al^{M1}+Cr+Ti+Fe^{3+})-K-Na-$

Table 1
The chemical compositions clinopyroxenes from garnet–pyroxene silicate rocks of the Kumdy-Kol Mine, Kokchetav massif

Generation	K-*Cpx*1							
Sample	Kum-39	Kum-40	Kum-40	Kum-40	Kum-40	Kum-02	Kum-02	Kum-02
Spot	L_A3	L_A1	L_A2	40-8-1	40-8-2	3058	3057	2179
SiO_2	51.39	50.43	50.54	50.74	50.94	51.40	51.61	51.04
TiO_2	0.06	0.15	0.16	0.13	0.11	0.03	0.01	0.03
Al_2O_3	0.65	1.42	1.48	2.12	0.74	1.16	1.24	1.13
FeO	17.91	17.21	17.31	16.90	16.65	14.10	14.11	14.45
MnO	0.38	0.48	0.51	0.33	0.53	0.35	0.14	0.32
MgO	6.92	6.91	6.85	6.87	7.46	9.15	8.91	9.04
CaO	21.94	22.65	22.92	21.40	22.07	22.55	22.56	22.70
Na_2O	0.16	0.12	0.10	0.35	0.24	0.15	0.32	0.19
K_2O	0.57	0.50	0.45	1.09	0.72	1.11	1.10	1.10
Total	99.98	99.87	100.32	99.93	99.45	100.00	100.00	100.00
Cations ratios (per 6 oxygens)								
Si	2.007	1.973	1.969	1.977	1.996	1.982	1.988	1.974
Ti	0.002	0.004	0.005	0.004	0.003	0.001	0.000	0.001
Al	0.030	0.065	0.068	0.097	0.034	0.053	0.056	0.052
Fe	0.585	0.563	0.564	0.550	0.545	0.454	0.454	0.467
Mn	0.013	0.016	0.017	0.011	0.017	0.011	0.005	0.010
Mg	0.403	0.403	0.398	0.399	0.435	0.526	0.511	0.521
Ca	0.918	0.949	0.957	0.893	0.926	0.931	0.930	0.940
Na	0.012	0.009	0.008	0.026	0.018	0.011	0.024	0.014
K	0.028	0.025	0.022	0.054	0.036	0.055	0.054	0.054
Results of calculation								
$X_{Mg}=Mg/(Mg+Fe)$	0.411	0.423	0.420	0.430	0.454	0.564	0.556	0.566
Fe^{3+}	0.007	0.014	0.014	0.022	0.022	0.048	0.046	0.067
Al^{T}	0.000	0.027	0.031	0.023	0.004	0.018	0.012	0.026
Al^{M1}	0.030	0.038	0.037	0.074	0.030	0.034	0.044	0.026
K + Na	0.040	0.034	0.030	0.081	0.054	0.066	0.078	0.068
$Al^{M1}+Cr+Ti+Fe^{3+}$	0.039	0.057	0.056	0.100	0.055	0.083	0.090	0.093
$[K+Na+Ca+Mn]^{M2}$	0.971	0.999	1.003	0.984	0.998	1.009	1.013	1.019
$[Mg+Fe]^{M1}$	0.961	0.943	0.944	0.900	0.945	0.917	0.910	0.907
Mg^{M1}	0.395	0.399	0.396	0.387	0.429	0.517	0.506	0.513
Fe^{M1}	0.566	0.544	0.548	0.513	0.516	0.400	0.404	0.394
Mg^{M2}	0.008	0.003	0.001	0.012	0.006	0.009	0.005	0.008
Fe^{M2}	0.011	0.005	0.002	0.015	0.007	0.007	0.004	0.006
Total cations	3.997	4.007	4.007	4.011	4.011	4.024	4.023	4.033
[T]	2.007	2.000	2.000	2.000	2.000	2.000	2.000	2.000
[M1]	1.000	1.000	1.000	1.000	1.000	1.000	1.000	1.000
[M2]	0.990	1.007	1.007	1.011	1.011	1.024	1.023	1.033
Vacancies in [M2]	0.010	0.000	0.000	0.000	0.000	0.000	0.000	0.000

(continued on next page)

Table 1 (*continued*)

Generation	*Cpx*2 (with *Kfs* inclusion)			*Cpx*3		
Sample	Kum-02	Kum-39	Kum-39	Kum-39	Kum-2	Kum-39
Spot	2141	2221	2213	436	421	429
SiO_2	51.87	50.06	50.08	50.18	52.56	51.17
TiO_2	0.05	0.00	0.01	0.00	0.00	0.00
Al_2O_3	0.68	0.37	0.35	0.48	0.38	0.22
FeO	13.51	19.36	18.91	21.15	13.44	18.27
MnO	0.38	0.27	0.51	0.74	0.28	0.40
MgO	9.74	6.64	6.54	4.88	10.26	6.92
CaO	23.24	22.96	23.32	22.47	22.90	22.95
Na_2O	0.28	0.30	0.27	0.00	0.00	0.00
K_2O	0.24	0.05	0.02	0.10	0.18	0.00
Total	99.99	100.01	100.01	100.00	100.00	99.93
Cations ratios (per 6 oxygens)						
Si	1.989	1.976	1.977	1.995	2.006	2.003
Ti	0.001	0.000	0.000	0.000	0.000	0.000
Al	0.031	0.017	0.016	0.022	0.017	0.010
Fe	0.433	0.639	0.624	0.703	0.429	0.598
Mn	0.012	0.009	0.017	0.025	0.009	0.013
Mg	0.556	0.391	0.385	0.289	0.583	0.404
Ca	0.954	0.971	0.986	0.957	0.936	0.962
Na	0.021	0.023	0.020	0.000	0.000	0.000
K	0.012	0.002	0.001	0.005	0.009	0.000
Results of calculation						
$X_{Mg} = Mg/(Mg + Fe)$	0.574	0.396	0.396	0.291	0.576	0.403
Fe^{3+}	0.021	0.042	0.037	0.000	0.000	0.000
Al^{T}	0.011	0.017	0.016	0.005	0.000	0.000
Al^{M1}	0.020	0.000	0.000	0.018	0.017	0.010
K + Na	0.033	0.025	0.021	0.005	0.009	0.000
$Al^{M1} + Cr + Ti + Fe^{3+}$	0.042	0.042	0.037	0.018	0.017	0.012
$[K + Na + Ca + Mn]^{M2}$	1.000	1.005	1.024	0.987	0.954	0.976
$[Mg + Fe]^{M1}$	0.958	0.958	0.963	0.982	0.983	0.988
Mg^{M1}	0.550	0.379	0.381	0.286	0.566	0.398
Fe^{M1}	0.408	0.579	0.582	0.696	0.416	0.590
Mg^{M2}	0.006	0.012	0.004	0.003	0.017	0.006
Fe^{M2}	0.005	0.018	0.005	0.007	0.012	0.008
Total cations	4.010	4.028	4.026	3.996	3.989	3.993
[T]	2.000	1.993	1.993	2.000	2.006	2.003
[M1]	1.000	1.000	1.000	1.000	1.000	1.000
[M2]	1.010	1.035	1.033	0.996	0.983	0.990
Vacancies in [M2]	0.000	0.000	0.000	0.004	0.017	0.010

Al^{IV}. If the *Esk* component is indeed present, the excess cations in M1 should be in positive correlation with vacancies $\square^{M2}$ in the proportion 2:1.

Using this scheme, all analyses were recalculated to the end-member compositions to check the concentration of *Esk* in both *Cpx*1 and *Cpx*2. If *Cpx*1 is a potential source of silica for producing the *Kfs* blebs + *Cpx*2, both the *Esk* and K-*Jad* components occur in *Cpx*1. In other words, excess cations in the M1 site must correlate with vacancies in the M2 site in proportion 2:1. As mentioned above, some potassium in *Cpx*1 is compensated in the M1 site by other Fe^{3+}, Cr, and Ti, while the rest is $KAlSi_2O_6$ end-member. By attributing all other cations as possible end-mem-

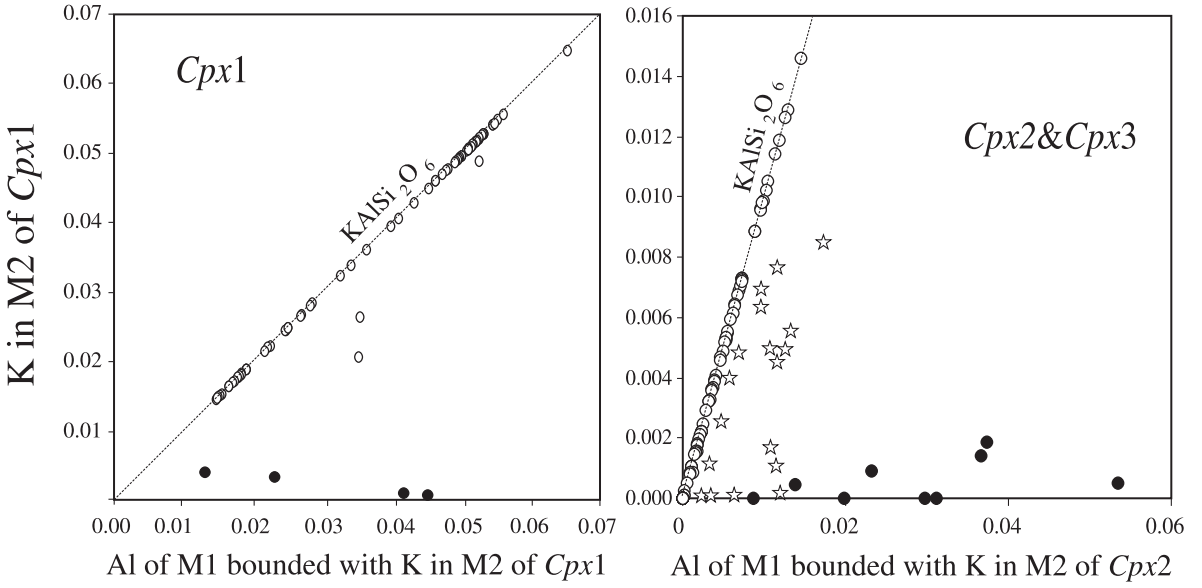

Fig. 4. Correlation between K and $Al^{VI} = Al^{M1} - Al^{T} - (Na + Fe^{3+} + 2Ti + Cr)$ in K-*Cpx* and suggesting predominantly isomorphic substitution in the solid solution $(Fe,Mg)Si_2O_6 - KAlSi_2O_6$. Open circles represent data points of *Cpx* from Fe-rich, diamond-free, coarse-grained *Grt-Cpx* rocks from the Kumdy-Kol Mine, the Kokchetav Complex; the closed circles reflect analyses from marble collected from the same Mine (see Table 1 in Zhu's paper). It is clearly seen that all closed circles differ significantly from the $(Fe,Mg)Si_2O_6 - KAlSi_2O_6$ solid solution, as well as from other data points (open circles). *Cpx*1: inclusions of euhedral *Cpx*1 in garnet; *Cpx*2: matrix clinopyroxene containing *Kfs* blebs. Open circles represent data points of *Cpx* from silicate rock (Perchuk et al., 1996, 2002), closed circles represent data points of *Cpx* from marble (Zhu, 2003); asterisks reflect rims of the *Cpx*2 grains from the *Grt-Cpx* rocks (see Fig. 6, *Cpx*3). Methods of calculation are discussed in the text.

bers (hedenbergite, diopside, jadeite, aegerine and negligible amount of *Tsch*) in *Cpx*1 at $Si + Al^{IV} = 2$, an excellent positive correlation of potassium with Al^{VI} in M1 in the *Cpx*1 was found (Fig. 4). Fig. 4a illustrates that, apart from potassium jadeite, $KAlSi_2O_6$, is the only end-member that contains Al in the M1 site of *Cpx*1, an indication that no *Esk* component is present in *Cpx*1. Therefore, the *Kfs* blebs cannot be formed by reaction (2) in the silicate rocks because of absence of the *Esk* component in *Cpx*1. Because the maximal content of potassium in *Cpx*2 is similar to minimal content in *Cpx*1 (Perchuk et al., 2002), a K–Al diagram for *Cpx*2 (Fig. 4b) demonstrates perfect correlation of K with Al for centers and cores, while compositions of rims are characterized by deviation from the K = Al line. This deviation suggests the presence of the *Esk* end-member in *Cpx*2. Both *Cpx*1 (inclusions in *Grt*) and *Cpx*2 (Cpx with blebs) from marble, used by Zhu (2003), are plotted in Fig. 4 for comparison. The comments on Fig. 4a are extra, while diagram b in this figure needs the special discussion that will be done in a corresponding section of this paper. This relationship suggests the presence of some amount of the *Esk* component but no vacancies in the M2 site. However, the average number of cations in this site is about of 1.01, with an average occupation of the M2 site of about of 0.99. The T position of *Cpx*2 from silicate rock is almost totally occupied by Si (average value from 107 analyses is about 1.99). This suggests presence of negligible amount of the *Tsch* in the *Cpx*2. This is further evidence for the displacement of reaction (2) to the left side for *Cpx*2 from silicate rocks. All these chemical evidence are supported by the presence of the *Kfs* blebs in garnet (Fig. 2a), which cannot be the products of the *Cpx*1 exsolution.

No potassium is present in *Cpx*3. This is practically pure salite that crystallized simultaneously with garnet of a composition different from *Grt*1 by containing a more andradite end-member, suggesting that final crystallization of the rock took place close to the Earth's surface.

4. *Cpx* from marble

Figs. 3 and 4 clearly illustrate that the *Cpx* from marble are compositionally different from those of the *Grt-Cpx* silicate rocks. In addition to the higher Ca (Fig. 3), all *Cpx* from marbles show higher Mg number ($X_{Mg}^{Cpx}=0.86-0.94$) at very low potassium (Fig. 4). As mentioned above, in order to produce the *Kfs* blebs by reaction (2), primary K-*Cpx* must contain (1) distinct amount of potassium and (2) corresponding concentration of the *Esk* molecule, while *Cpx*2 containing the *Kfs* blebs must be potassium-free and *Tsch*-rich. However, both the *Cpx*1 (inclusions) and *Cpx*2 (matrix with blebs) described by Zhu are similar in compositions (Fig. 3 in their paper). In addition, there is no correlation between K and Al either in *Cpx*1 or *Cpx*2. Fig. 4 clearly demonstrates that *Kfs* blebs cannot be produced from the potassium-free *Cpx*1 in marble. But perhaps *Cpx*1 in marble contains *Esk* component, allowing the production of *Kfs* blebs by intracrystalline reaction (2). The M2 site of *Cpx*1 from marble is almost totally occupied by Ca, Na, K, and Mn (in *Cpx*1 this total reaches 1.004). Zhu and Ogasawara do not state how the *Esk* content was calculated. Nevertheless, if this end-member occurred in *Cpx*1 before exsolution, *Cpx*2 as a product of reaction (2), must be undersaturated in Si, because of the *Tsch* content. However, an average crystallochemical formula of *Cpx*2 in Table 1 of Zhu's paper shows Si = 2.001. It may be that single compositions of *Cpx*2 form a trend after reaction (2), suggesting an increase of the *Tsch* component at the expense of the *Esk* component? In this case, a negative correlation between Si and the *Esk* component Al^{M1} should be observed in *Cpx*2 from marble. However, such a correlation is not a characteristic of this *Cpx* (Fig. 5). Moreover, Fig. 5 shows a weak positive correlation between these compositions of all *Cpx*, in which $Al^{M1}>Na+K$. This suggests an increase of the *Esk* component in *Cpx*2 and *Cpx*3, contradicting the shift of reaction (2) to the right. Thus, *Cpx*2 from marble shows a standard content of Si and no negative correlation between Si and Al^{M1}, while *Cpx*1 has no vacancies in M2, i.e. no *Esk* component in the solid solution.

5. Discussion and conclusions

Compositional differences preclude the direct comparison of rocks and minerals described by us with those described by Zhu (2003). Most *Cpx* inclusions in garnets from the *Grt-Cpx* rocks are potassium-rich, while those from marble are potassium-free. No *Esk* component is found to pose as a possible donor of silica in *Cpx*1 of the silicate rocks (Table 1). If a rock does not

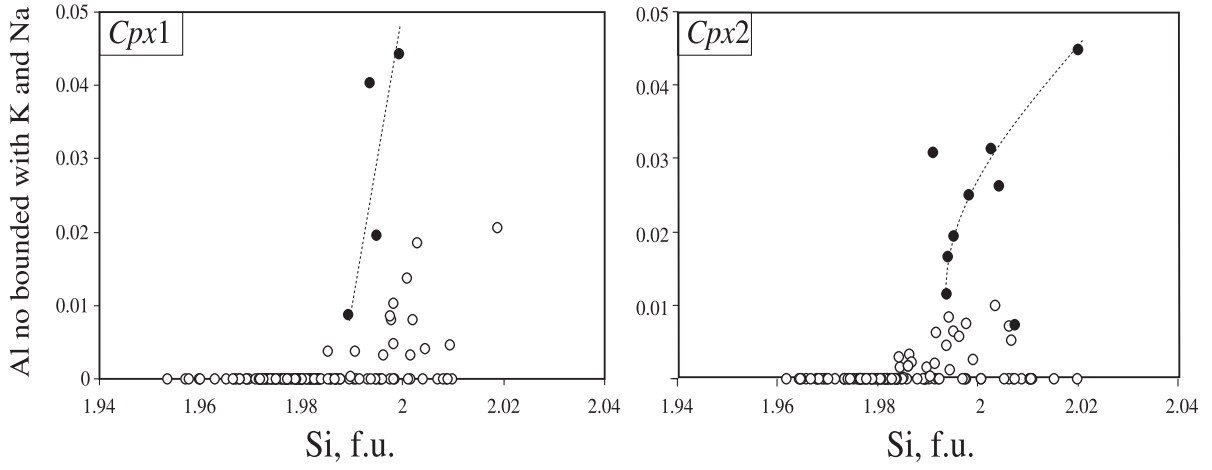

Fig. 5. Diagrams showing no negative correlation between content of Si and the rest of Al^{M1} presumably bounded in *Tsch* component as a product of reaction (2). Open circles represent data points of *Cpx* from silicate rock (Perchuk et al., 1996; 2002); Closed circles represent data points of *Cpx* from marble (Zhu, 2003).

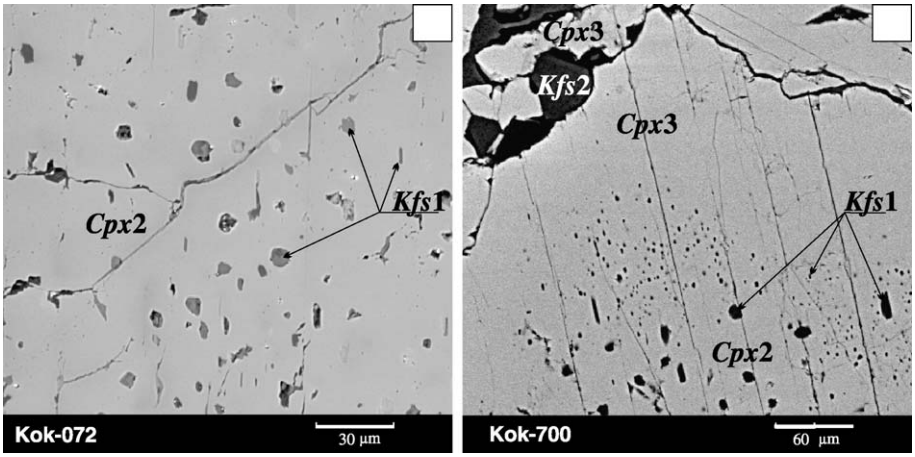

Fig. 6. Backscattered images of *Kfs* blebs showing no systematic shapes or compositional distributions in *Cpx*2 and they do not occur along *Cpx*2 cleavage. Diamond-free coarse-grained *Grt-Cpx* rock from the Kumdy-Kol Mine, the Kokchetav Complex.

contain primary potassium- and *Esk*-bearing *Cpx* (*Cpx*1), there is no chance for it to contain *Kfs* blebs as an exsolution product. No *Tsch* component is present in *Cpx*2 from the silicate rock (Table 1). Since *Cpx*2, as a possible exsolution product of reaction (2) does not contain *Tsch*, therefore the reaction (2) cannot reflect a mechanism of the formation of *Kfs* blebs in *Cpx*2.

Fig. 4b demonstrates small (0.005) but systematic deviation of 19 of 107 *Cpx*2 data points from the K = Al line for the Ca(Fe, Mg)Si_2O_6–$KAlSi_2O_6$ solid solution. All these data relate to rims of the *Cpx*2 grains from *Grt-Cpx* rocks (*Cpx*3). This deviation suggests extra Al is bonded neither with K, nor with some other components from the M1 and M2 sites. The only explanation can be that we have to assume the existence of "clinocorundum" $Al_2Al_2O_6$ in M2 of *Cpx*2 from the silicate rock. However, this component cannot be a characteristic of the *Cpx*2 solid solution from marble because both M1 and M2 are oversaturated by cations. For example, the total of Ca + Na + K in the M2 site in average *Cpx*2 from marble equals 1.004. Even if we assume that the extra Al represents the *Esk* end-member in *Cpx*2, it indicates the displacement of reaction (2) to the left, i.e. consumption of the *Kfs* blebs rather than their formation.

Thus, the data presented above demonstrate the error produced by comparison of the *Kfs* blebs in the rocks of different origin. The saying goes: "How misleading appearances are sometimes," sighed a little hedgehog getting off the shoe brush. Our model of the crystallization of *Kfs* blebs in the *Cpx*2 from a silicate liquid is the only alternative unless the *Kfs* blebs (see Fig. 6) form after the reaction, involving a fluid:

$$\mathrm{Ca(Fe,Mg)Si\,O_6} \cdot n\mathrm{KAlSi_2O_6}(\text{in } Cpx) + [\mathrm{SiO_2}]_{\mathrm{fluid}} \Rightarrow n\mathrm{KAlSi_3O_8} + \mathrm{Ca(Fe,Mg)Si_2O_6} \quad (3)$$

In addition to alkalis, such a mantle-derived fluid is rich in silica (Navon et al., 1988; Schrauder and Navon, 1994; Israeli et al., 1998). Because sanidine is not stable at a pressure above 60 kbar (e.g., Urakawa et al., 1994), we suggested that reaction (1) takes place at relatively low pressures (Perchuk et al., 2002), outside of field stability of the K-*Cpx*. At present, however, no experimental data exist for (1), (2) and (3). Hopefully, these data will appear in the near future.

References

Bindi, L., Safonov, O.G., Yapaskurt, V.O., Perchuk, L.L., Menchetti, S., 2003. Ultrapotassic Cpx from the Kumdy-Kol microdiamond mine, Kokchetav Complex, Kazakhstan: occurrence, composition and crystal–chemical characterization. Am. Mineral. 88, 464–468.

Dobretsov, N.L., Kochkin, Yu.N., Krivenko, A.P., Kutolin, V.A., 1971. Rock-Forming Pyroxenes Nauka Press, Moscow. 452 pp.

Edgar, A.D., Mitchell, R.H., 1997. Ultra high pressure–temperature melting experiments on an SiO_2-rich lamproite from Smoky Butte, Montana: derivation of siliceous lamproite magmas from enriched sources deep in the continental mantle. J. Petrol. 38, 457–477.

Edgar, A.D., Vukadinovic, D., 1993. Potassium-rich Cpx in the mantle: an experimental investigation of K-rich lamproite up to 60 kbar. Geochim. Cosmochim. Acta 57, 5063–5072.

Israeli, E., Schrauder, M., Navon, O., 1998. On the connection between fluids and mineral inclusions in diamonds. Extended Abstracts, 7th International Kimberlite Conference, Cape Town, pp. 352–354.

Luth, R.W., 1997. Experimental study of the system phlogopite–diopside from 3.5 to 17 GPa. Am. Mineral. 82, 1198–1209.

Mitchell, R.H., 1995. Melting experiments on a sanidine–phlogopite lamproite at 4–7 GPa and their bearing on the source of lamproitic magmas. J. Petrol. 36, 1455–1474.

Navon, O., Hitcheon, I.D., Rossman, G.R., Wasserburg, G.J., 1988. Mantle-derived fluids in diamond microinclusions. Nature 325, 784–789.

Perchuk, L.L., Yapaskurt, V.O., 1998. Mantle-derived ultrapotassic liquids. Russian Geology and Geophysics 39, 1746–1755.

Perchuk, L.L., Yapaskurt, V.O., Okay, A., 1995. Comparative petrology of diamond-bearing metamorphic complexes. Petrology 3, 238–276.

Perchuk, L.L., Sobolev, N.V., Yapaskurt, V.O., Shatsky, V.S., 1996. Relics of potassium-bearing pyroxenes from diamond-free pyroxene-garnet rocks of the Kokchetav massif, northern Kasakhstan. Dokl. Ross. Akad. Nauk, Earth Sci. 348, 790–795.

Perchuk, L.L., Safonov, O.G., Yapaskurt, V.O., Barton, J.M., 2002. Crystal-melt equilibria involving potassium-bearing Cpx as indicator of mantle-derived ultrahigh-potassic melts: an analytical review. Lithos 60, 89–112.

Reid, A.M., Brown, R.W., Dawson, J.B., Whitfield, G.G., Siebert, J.C., 1976. Garnet and pyroxene compositions in some diamondiferous eclogites. Contrib. Mineral. Petrol. 58, 203–220.

Safonov, O.G., Matveev, Yu.A., Litvin, Yu.A., Perchuk, L.L., 2002. Experimental study of some joints in the system $CaMgSi_2O_6$–$(Ca,Mg)_3Al_2Si_3O_{12}$–$KAlSi_2O_6$–$K_2(Ca,Mg)(CO_3)_2$ at 5–7 GPa in relation to the Genesis of *Grt-Cpx*–carbonate rocks of the Kokchetav Complex, Northern Kazakhstan. Petrology 10 (6), 519–539.

Schrauder, M., Navon, O., 1994. Hydrous and carbonatitic mantle fluids in fibrous diamonds from Jwaneng, Botswana. Geochim. Cosmochim. Acta 58, 761–771.

Sobolev, N.V., Shatsky, V.S., 1990. Diamond inclusions in garnets from metamorphic rocks: a new environment for diamond formation. Nature 343, 742–746.

Urakawa, S., Kondo, T., Igawa, N., Shimomura, O., Ohno, H., 1994. Synchrotron radiation study on the high-pressure and high-temperature phase relations of $KAlSi_3O_8$. Phys. Chem. Miner. 21, 387–391.

Zhang, R.Y., Liou, J.G., Ernst, W.G., Coleman, R.G., Sobolev, N.V., Shatsky, V.S., 1997. Metamorphic evolution of diamond-bearing and associated rocks from the Kokchetav Massif, northern Kazakhstan. J. Metamorph. Geol. 13, 479–496.

Zhu, Y., 2003. Comments on: "Crystal-melt equilibria involving potassium-bearing clinopyroxene as indicator of mantle-derived ultrahigh-potassic liquids: an analytical review" by Perchuk, L.L., Safonov, O.G., Yapaskurt, V.O., Barton Jr., J.M. [Lithos 60 (2002) 89–111]: K-feldspar in metamorphic clinopyroxene, from exsolution to potassium replacement. Lithos. this issue.